ВИРОБНИЦТВО ОВТ

УДК 53.088:62 – 754.2 (045)

V. Apostolyuk

Aerospace Systems Faculty, National Technical University of Ukraine "KPI", Kyiv

DEMODULATED DYNAMICS AND OPTIMAL NOISE FILTERING FOR CORIOLIS VIBRATORY GYROSCOPES

Analysis of the Coriolis vibratory gyroscopes sensitive element dynamics in terms of the amplitude-phase variables led to the proper transfer functions of such inertial sensors, where angular rate is an input. Obtained transfer functions were simplified for the several special cases and then used to derive poles, amplitude, and phase responses of CVG. Performance of the simplified transfer functions is also analyzed and compared to the accurate numerical model of the sensitive elements dynamics. Obtained transfer functions were then used to derive static (Wiener) and adaptive (Kalman) optimal filters of stochastic sensor noise for Coriolis vibratory gyroscopes.

Key words:: *Coriolis vibratory gyroscope, sensitive element dynamics, micromechanical gyroscope, optimal filtering, sensor noise.*

Introduction

Coriolis vibratory gyroscopes (CVGs) received significant amount of interest from the both scientific and engineering communities in view of the possibility to fabricate sensitive elements of such gyroscopes in miniature form by using modern microelectronic mass-production technologies. In this case CVGs are frequently referred to as MEMS (Micro-Electro-Mechanical-Systems) gyroscopes [1]. Apart from numerous civil applications this type of inertial sensors is also considered as a key element in guidance systems for different kinds of munitions due to its low-cost and high survivability, which is essential for the combat systems. Being based on sensing of Coriolis acceleration due to the rotation in oscillating structures, CVGs have a lot more complicated mathematical models, comparing to the conventional types of gyroscopes. One of such complication is a result of the useful signal proportional to the external angular rate being modulated with the intentionally excited primary oscillations [2-4]. From the mathematical modeling point of view, this leads to necessity to "demodulate" the solution in terms of the sensitive element displacements to obtain practically feasible insights into CVG dynamics and errors. From the control systems point of view, conventional representation of CVGs incorporates primary oscillation excitation signal as an input to the dynamic system, and unknown angular rate as a coefficients of its transfer functions [4]. As a result, dynamics of CVGs has been analyzed mainly in steady state, while transient process analysis, for example, has been omitted due to its apparent complexity.

This paper describes new method of CVG dynamics analysis by means of complex amplitude-phase variables, which enables having angular rate as an input to the dynamic system. As a result, new system transfer functions of CVG in demodulated signals were derived and used for analysis of its dynamics.

CVG motion equations

Sensitive element of the most CVGs can be represented as a massive element (proof mass m_2 in Fig. 1) attached to the basis by means of set of springs and the decoupling frame m_1.

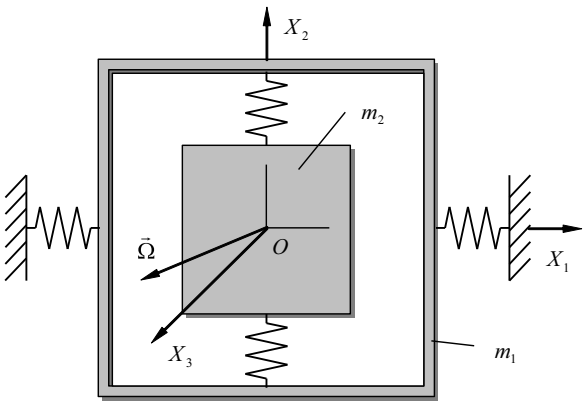

Fig. 1. **Generalised CVG sensitive element**

Here springs may allow either translational or rotational motion of the proof mass and decoupling

frame. Primary oscillations of the sensitive element are excited along the axis X_1, and secondary oscillations of the proof mass due to the angular rate $\vec{\Omega}$ are detected along the axis X_2.

In the most generalized form, motion equations of the CVG sensitive element both with translational and rotational motion could be represented in the following form:

$$\begin{cases} \ddot{x}_1 + 2\zeta_1 k_1 \dot{x}_1 + (k_1^2 - d_1\Omega^2)x_1 + \\ g_1\Omega\dot{x}_2 + d_3\dot{\Omega}x_2 = q_1 \\ \ddot{x}_2 + 2\zeta_2 k_2 \dot{x}_2 + (k_2^2 - d_2\Omega^2)x_2 \\ -g_2\Omega\dot{x}_1 - \dot{\Omega}x_1 = q_2 \end{cases} \quad (1)$$

Here x_1 and x_2 are the generalized coordinates that describe primary (excited) and secondary (sensed) motions of the sensitive element respectively, k_1 and k_2 are the corresponding un-damped natural frequencies, ζ_1 and ζ_2 are the dimensionless relative damping coefficients, Ω is the measured angular rate, which is orthogonal to the axes of primary and secondary motions, q_1 and q_2 are the generalized accelerations due to the external forces acting on the sensitive element. The remaining dimensionless coefficients are different for the sensitive elements exploiting either translational or rotational motion. For the translational sensitive element they are $d_1 = d_2 = 1$, $d_3 = m_2/(m_1 + m_2)$, $g_1 = 2m_2/(m_1 + m_2)$, $g_2 = 2$, where m_1 and m_2 are the masses of the outer frame and the internal massive element [5]. In case of the rotational motion of the sensitive element, these coefficients are the functions of different moments of inertia (for greater details see [5] as well). In the presented above motion equations, the angular rate is included as an unknown and variable coefficient rather than an input to the double oscillator system. Conventional control systems representation of such a dynamic system is shown in Fig. 2.

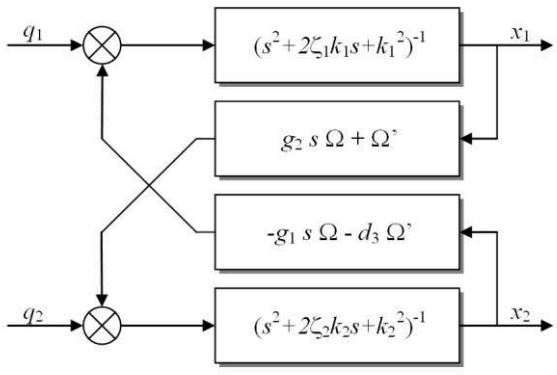

Fig. 2. **Conventional representation of CVG dynamics in control systems**

In order to identify the angular rate one must detect secondary oscillations of the sensitive element and measure its amplitude, which is approximately directly proportional to the angular rate, and phase, which gives the sign. Compatible with the most control problems CVG dynamics representation should have the unknown angular rate as an input and its measured value as an output.

In order to make the equations (1) suitable for to the transient process analysis we must make the following assumptions: angular rate is small comparing to the primary and secondary natural frequencies so that

$$k_1^2 >> d_1\Omega^2,\ k_2^2 >> d_2\Omega^2, \quad (2)$$

and rotational and Coriolis accelerations acting along primary oscillation axis are negligible in comparison to the accelerations from driving forces

$$g_1\Omega\dot{x}_2 + d_3\dot{\Omega}x_2 << q_1. \quad (3)$$

Taking into considerations assumptions (2) and (3), motions equations (1) could be simplified to the following form:

$$\begin{cases} \ddot{x}_1 + 2\zeta_1 k_1 \dot{x}_1 + k_1^2 x_1 = q_1 \\ \ddot{x}_2 + 2\zeta_2 k_2 \dot{x}_2 + k_2^2 x_2 = g_2\Omega\dot{x}_1 + \dot{\Omega}x_1. \end{cases} \quad (4)$$

Here we also assumed that no external driving forces are affecting the secondary oscillations, which means that $q_2 = 0$.

System of equations (4) is now perfectly suitable for further transformations towards the desired representation in terms of the unknown angular rate.

Amplitude-phase motion equations

As has been shown in [5], by means of a proper chosen phase shift of the excitation voltage applied to the sensitive element, the excitation force could be shaped to the perfect harmonic form. Using exponential representation of complex numbers, such a driving force q_1 could be represented as

$$q_1 = q_{10}\sin(\omega t) = \mathrm{Im}\{q_{10}e^{j\omega t}\}. \quad (5)$$

Here ω is the excitation frequency given in radians per second, q_{10} is the constant excitation acceleration amplitude. Non-homogeneous solutions of the motion equations (1) or (4) for primary and secondary oscillations are represented in a similar form

$$\begin{aligned} x_1 &= \mathrm{Im}\{A_1(t)e^{j\omega t}\},\ A_1 = A_{10}(t)e^{j\varphi_{10}(t)}, \\ x_2 &= \mathrm{Im}\{A_2(t)e^{j\omega t}\},\ A_2 = A_{20}(t)e^{j\varphi_{20}(t)}, \end{aligned} \quad (6)$$

where A_{10} and A_{20} are the primary and secondary oscillation amplitudes, φ_{10} and φ_{20} are the corresponding phase shifts relatively to the excitation force. Although

these quantities are real (non-complex), they are combined in complex amplitude-phase variables A_1 and A_2.

Substituting expressions (5) and (6) into equations (4) results in the following motions equations in terms of the complex amplitude-phase variables rather than real generalized coordinates:

$$\begin{cases} \ddot{A}_1 + 2(\zeta_1 k_1 + j\omega)\dot{A}_1 + (k_1^2 - \omega^2 + 2j\omega k_1\zeta_1)A_1 = \\ = q_{10}, \\ \ddot{A}_2 + 2(\zeta_2 k_2 + j\omega)\dot{A}_2 + (k_2^2 - \omega^2 + 2j\omega k_2\zeta_2)A_2 = \\ = (j\omega g_2\Omega + \dot{\Omega})A_1 + g_2\dot{A}_1\Omega. \end{cases} \quad (7)$$

Equations (7) describe variations of the amplitude and phase of the primary and secondary equations in time with respect to the unknown non-constant angular rate $\Omega = \Omega(t)$. This allows conducting analysis of the Coriolis vibratory gyroscope dynamics without constraining the angular rate to be constant or slowly varying.

Analyzing system (7), one can see that the first equation can be solved separately from the second one. After homogeneous solutions of the first equation faded out, only non-homogenous solution remains. In this case, amplitude of the primary oscillations is

$$A_1 = \frac{q_{10}}{k_1^2 - \omega^2 + 2jk_1\zeta_1\omega}, \quad (8)$$

and it is constant in time, yielding $\ddot{A}_1 = \dot{A}_1 = 0$. Indeed, most of the time measurements of the angular rate are performed when primary oscillations have already settled. As a result, only equation for the secondary oscillations remains, in which the complex primary amplitude A_1 is just a constant parameter given by (8):

$$\begin{aligned} &\ddot{A}_2 + 2(\zeta_2 k_2 + j\omega)\dot{A}_2 + (k_2^2 - \omega^2 + 2j\omega k_2\zeta_2)A_2 = \\ &= (j\omega g_2\Omega + \dot{\Omega})A_1. \end{aligned} \quad (9)$$

Equation (9) now describes amplitude-phase of the secondary oscillations with respect to the *settled* primary oscillations.

System transfer functions

Having CVG sensitive element motion equation in the form (9), allows analysis of its transient processes in amplitudes and phases with respect to arbitrary angular rates applied to the system. Application of the Laplace transformation to the equation (9) with respect to zero initial conditions for all time-dependent variables results in the following expressions:

$$\begin{aligned} &[(s + j\omega)^2 + 2\zeta_2 k_2(s + j\omega) + k_2^2]A_2(s) = \\ &= A_1[s + jg_2\omega]\Omega(s). \end{aligned} \quad (10)$$

Solution of the algebraic equation (10) for the secondary amplitude-phase Laplace transform is

$$A_2(s) = \frac{A_1 \cdot (s + jg_2\omega)}{(s + j\omega)^2 + 2\zeta_2 k_2(s + j\omega) + k_2^2}\Omega(s). \quad (11)$$

Considering the angular rate as an input, the system transfer function for the secondary amplitude-phase is

$$\begin{aligned} W_2(s) &= \frac{A_2(s)}{\Omega(s)} = \\ &= \frac{A_1(s + jg_2\omega)}{(s + j\omega)^2 + 2\zeta_2 k_2(s + j\omega) + k_2^2} = \\ &= \frac{q_{10}(s + jg_2\omega)}{[(s + j\omega)^2 + 2\zeta_2 k_2(s + j\omega) + k_2^2]} \times \\ &\times \frac{1}{[k_1^2 - \omega^2 + 2j\omega k_1\zeta_1]}. \end{aligned} \quad (12)$$

One should note that transfer function (12) has complex coefficients, which results in the complex system outputs as well. Although it is somewhat unusual, it still enables us to analyse CVG dynamics and transient processes due to the angular rate in an open-loop dynamic system.

Amplitude and phase responses

In order to calculate the amplitude response of the system using transfer function (12), Laplace variable s must be replaced with the Fourier variable $j\lambda$, where λ is the frequency of the angular rate oscillations:

$$\begin{aligned} W_2(j\lambda) &= \frac{jq_{10}(\lambda + g_2\omega)}{[k_2^2 - (\lambda + \omega)^2 + 2j\zeta_2 k_2(\lambda + \omega)]} \times \\ &\times \frac{1}{[k_1^2 - \omega^2 + 2j\omega\zeta_1 k_1]}. \end{aligned} \quad (13)$$

Absolute value of the complex function (13) is the amplitude response of the secondary oscillations amplitude to the harmonic angular rate, and the corresponding phase of the complex function is the phase response [5]:

$$\begin{aligned} A(\lambda) &= \frac{q_{10}(\lambda + g_2\omega)}{[(k_2^2 - (\lambda + \omega)^2)^2 + 4\zeta_2^2 k_2^2(\lambda + \omega)^2]^{\frac{1}{2}}} \times \\ &\times \frac{1}{[(k_1^2 - \omega^2)^2 + 4\zeta_1^2 k_1^2\omega^2]^{\frac{1}{2}}}, \\ \varphi(\lambda) &= \tan^{-1}\{\Delta^{-1}[k_2^2 - (\lambda + \omega)^2][k_1^2 - \omega^2] - \\ &- \Delta^{-1} 4k_1 k_2\zeta_1\zeta_2\omega(\lambda + \omega), \\ \Delta &= 2[k_2\zeta_2(\lambda + \omega)(k_1^2 - \omega^2) + \\ &+ k_1\zeta_1\omega(k_2^2 - (\lambda + \omega)^2)]. \end{aligned} \quad (14)$$

One should note that, assuming constant angular rate ($\lambda = 0$) in the expressions (14), the well known expressions ([4]) for the amplitude and phase of the secondary oscillations could be obtained.

Analysis of the expressions (14) shows that effect from the oscillating angular rate is practically equivalent to shift of the excitation frequency ω by the frequency λ of the angular rate. This causes CVGs, especially those with high Q-factor, to loose its resonant tuning, which in turn results in significant variation of its scale factor (dynamic error) and thus limited bandwidth.

System poles and slow motion

Both stability and unit-step transient process quality depend on position of the system poles in the real-imaginary plane. Poles of the transfer function (12) are as follows:

$$s_{1,2} = -k_2\zeta_2 \pm jk_2\sqrt{1-\zeta_2^2} - j\omega . \qquad (15)$$

Analysing expression (15), it is easy to see that CVGs are inherently stable. Indeed, if the relative damping coefficient $\zeta_2 \le 1$, then real parts of the poles are $-k_2\zeta_2 < 0$. If the relative damping coefficient $\zeta_2 > 1$, then real parts are $-k_2(\zeta_2 \pm \sqrt{\zeta_1^2 - 1}) < 0$.

One should note, that each of the poles (15) corresponds to different kinds of motion of the sensitive element in terms of the amplitude-phase variables. Most essentially, actual amplitude of the secondary oscillations is mainly defined by the low frequency pole, while effect from the high frequency pole can be neglected, since it will be removed during demodulation process. In other words, predominant behaviour is a slow variation of the amplitude and phase. Neglecting the second order derivative in the equation (9) yields

$$2(\zeta_2 k_2 + j\omega)\dot{A}_2 + (k_2^2 - \omega^2 + 2j\omega k_2\zeta_2)A_2 = \\ = (j\omega g_2\Omega + \dot{\Omega})A_1,$$

and the corresponding angular rate transfer function becomes

$$W_2(s) = \frac{q_{10}(s + jg_2\omega)}{[2\zeta_2 k_2 s + k_2^2 - \omega^2 + j2\omega(\zeta_2 k_2 + s)]} \times \\ \times \frac{1}{[k_1^2 - \omega^2 + 2j\omega k_1\zeta_1]}. \qquad (16)$$

Single pole of this transfer function is

$$s_1 = -\frac{k_2^2 - \omega^2 + 2j\omega\zeta_2 k_2}{2(\zeta_2 k_2 + j\omega)} . \qquad (17)$$

Complex transfer function (16) is simpler in comparison to the function (12) and could replace it in certain specific problems when slow oscillations analysis is required.

Real and imaginary transfer functions

While simulating dynamics of CVG based on the complex amplitude-phase transfer functions (12) or (16) one could have problems dealing with complex coefficients of these transfer functions (for example, while simulating CVG using Simulink/Matlab). One way to avoid this problem is to consider real and imaginary parts of complex amplitude as separate signals, which are then combined together to produce real amplitude and phase. In order to obtain transfer functions for such signals let us represent primary and secondary amplitudes as

$$A_1 = A_{1R} + jA_{1I}, \; A_2 = A_{2R} + jA_{2I} . \qquad (18)$$

Primary oscillations components can be easily found by means of substituting expressions (18) into formula (8) thus yielding

$$A_{1R} = \frac{q_{10}(k_1^2 - \omega^2)}{(k_1^2 - \omega^2)^2 + 4k_1^2\zeta_1^2\omega^2}, \\ A_{1I} = -\frac{2q_{10}j\omega k_1\zeta_1}{(k_1^2 - \omega^2)^2 + 4k_1^2\zeta_1^2\omega^2} . \qquad (19)$$

At the same time, substituting expressions (19) into the motion equation (9), and applying Laplace transformation with zero initial conditions gives

$$\begin{cases} (k_2^2 - \omega^2 + 2k_2\zeta_2 s + s^2)A_{2R}(s) - \\ - 2\omega(k_2\zeta_2 + s)A_{2I}(s) = (A_{1R}s - A_{1I}g_2\omega)\Omega(s), \\ (k_2^2 - \omega^2 + 2k_2\zeta_2 s + s^2)A_{2I}(s) + \\ + 2\omega(k_2\zeta_2 + s)A_{2R}(s) = (A_{1I}s + A_{1R}g_2\omega)\Omega(s). \end{cases} . \qquad (20)$$

Resolving algebraic system (20) for the unknown real and imaginary parts of the secondary complex amplitude results in

$$A_{2R}(s) = \frac{A_{1R}M_{RR}(s) + A_{1I}M_{RI}(s)}{P(s)}\Omega(s) , \\ A_{2I}(s) = \frac{A_{1R}M_{IR}(s) + A_{1I}M_{II}(s)}{P(s)}\Omega(s) . \qquad (21)$$

Here the numerator polynomials from the real and imaginary parts of primary amplitudes are given by the following expressions:

$$M_{RR}(s) = s(k_2^2 + 2k_2\zeta_2 s + s^2) - \\ - \omega^2(s - 2g_2(s + k_2\zeta_2)), \\ M_{RI}(s) = \omega[2s(s + k_2\zeta_2) - \\ - g_2(k_2^2 - \omega^2 + 2k_2\zeta_2 s + s^2)], \\ M_{II}(s) = 2\omega^2 g_2(s + k_2\zeta_2) + \\ + s(k_2^2 - \omega^2 + 2k_2\zeta_2 s + s^2)], \\ M_{IR}(s) = \omega[g_2(k_2^2 - \omega^2 + 2k_2\zeta_2 s + s^2) - \\ - 2s(s + k_2\zeta_2)], \\ P(s) = 4(s + k_2\zeta_2)^2\omega^2 + \\ + (k_2^2 - \omega^2 + 2k_2\zeta_2 s + s^2)^2. \qquad (22)$$

Obtained expressions (19), (21), and (22) allow analysis of CVG dynamics in control system without necessity to involve complex-valued signals.

Simplified transfer function and its accuracy

There is quite an important special case, when complex transfer functions transform to a simple real-valued one. Assuming equal primary and secondary natural frequencies ($k_1 = k_2 = k$), equal damping ratios ($\zeta_1 = \zeta_2 = \zeta$), primary resonance excitation ($\omega = k\sqrt{1-2\zeta^2}$), and constant angular rate ($\dot{\Omega} \approx 0$), one can easily obtain

$$A_{20} = \frac{g_2 q_{10}\sqrt{1-2\zeta^2}}{4\zeta k^2(1-\zeta^2)(s+k\zeta)}\Omega. \qquad (23)$$

In this case, secondary amplitude (23) is related to the input angular rate by means of the following transfer function

$$W_{20}(s) = \frac{A_{20}(s)}{\Omega(s)} = \frac{q_{10} g_2 \sqrt{1-2\zeta^2}}{4k^2\zeta(1-\zeta^2)(s+k\zeta)}. \qquad (24)$$

As one can see, the simplified CVG transfer function (24) describes a simple first-order system with exponential (non-oscillatory) transient process.

Finally, transfer function (24) relates angular rate to the secondary oscillations amplitude. However, more appropriate would be to consider transfer function relating unknown input angular rate to the measured angular rate, which can be easily obtained from (24) by dividing it on the steady state scale factor. The resulting transfer function is

$$W(s) = \frac{k\zeta}{s+k\zeta}. \qquad (25)$$

Somewhat qualitatively similar results were obtained from the different considerations in [6]. Needless to say, that possibility to use transfer functions (24) and (25) for "non-tuned" CVG as well is highly desired. Therefore let us evaluate accuracy of the function (24) in representing general case of CVG dynamics.

In order to do that, let us compare transient processes produced by the simplified transfer function and by a numerical solution of the equations (1) with subsequent demodulation. As a performance criterion the following integral function is used:

$$J(\delta k, \delta\zeta) = \int_0^T [A_{20}(t) - A_{20}^*(t)]^2 dt. \qquad (26)$$

Here $\delta k = k_2 / k_1$ is the ratio of the natural frequencies, $\delta\zeta = \zeta_2 / \zeta_1$ is the ratio of the relative damping ratios, $A_{20}^*(t)$ is the demodulated secondary amplitude produced by the "realistic" model.

Graphic plot of the functional (26) is shown below in the figure 3.

Here the central darker area corresponds to the perfectly tuned device ($\delta k = 1$, $\delta\zeta = 1$). One can see, that wide range of sensitive elements with varying ratio of the natural frequencies and ratio of relative damping still could be represented by the transfer function (24) with acceptably low integral error (26).

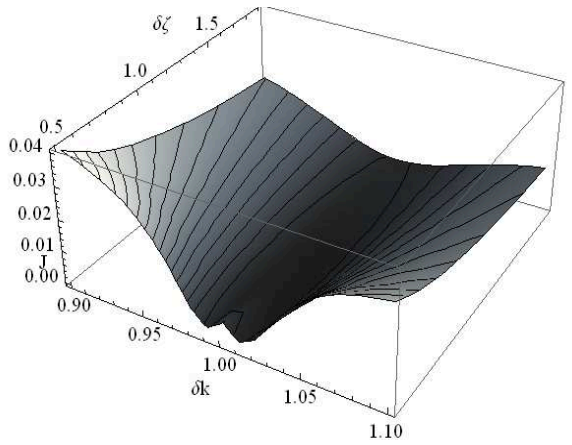

Fig. 3. **Integral error of the transient process representation**

Stochastic unobserved noises

Accuracy of CVG is usually limited by different kinds of noises and systematic errors. Especially micromachined kinds of CVG are essentially affected by a thermal mechanical noise [6, 7]. Performances of CVGs are affected by unobserved stochastic influences in two ways: as a "sensor noise", which is added to the output of the system, and as a "process noise" or disturbances, which are added to the input of the system. The latter could be also treated as "rate-like" disturbances. Such system is shown in the figure 4.

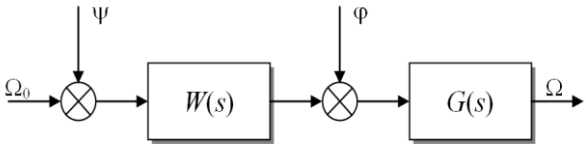

Fig. 4. **Process and sensor noises in CVG**

Here $W(s)$ is the system transfer function given by (25), ψ is the stochastic disturbance, φ is the sensor noise, $G(s)$ is the transfer function of a static optimal filter (yet to be derived), Ω_0 is the actual angular rate, Ω is the angular rate measured by the CVG with the filter, which in ideal case is equal to the actual angular rate Ω_0. Since in general disturbances are by no means different from the actual angular rate, let us therefore concentrate on the sensor noise removal.

Assuming that CVG is installed on a moveable object, such as aircraft or land vehicle, its power spectral density can be represented as

$$S_\Omega(s)=\frac{\sigma^2 B^2}{B^2-s^2}. \quad (27)$$

Here B is the moveable object bandwidth, and σ is the measure of the angular rate power factor.

Meanwhile, sensor noises can be assumed to be either a white noise like with the following power spectral density

$$S_\varphi(s)=\gamma^2\sigma^2, \quad (28)$$

or a high-pass noise

$$S_\varphi(s)=-\frac{\gamma^2\sigma^2 s^2}{B^2-s^2}. \quad (29)$$

Here γ is the noise-to-signal ratio. Power spectral densities (28) and (29) along with the angular rate power spectral density (27) cover most of the present in CVG cases of stochastic sensor noises. Nevertheless, other specific spectral densities can be taken into account and used in the presented below optimal filter synthesis procedure.

Optimal Wiener filter synthesis

General algorithm of the optimal filter synthesis for the system in Fig. 4 has been demonstrated in [8], with respect to the stationary stochastic sensor noise.

Error of the system is defined as a difference between the actual output of the system Ω and the ideal output, which is the given by the desired transformation $H(s)$ of the input as

$$\varepsilon=\Omega-H(s)\cdot\Omega_0.$$

It is also assumed that signals Ω and Ω_0 are the centered stochastic processes defined in terms of system transfer functions and known spectral densities of the input angular rate and sensors noises.

Performance criterion for the system is assumed to be in the form of the following functional:

$$J=E\{\varepsilon'\cdot\varepsilon\}=\frac{1}{j}\int_{-j\infty}^{j\infty}S_{\varepsilon\varepsilon}(s)ds. \quad (30)$$

Here $S_{\varepsilon\varepsilon}(s)$ is the error spectral density, which can be calculated from the system transfer functions and signal spectral densities using Wiener-Khinchin theorem [8] as follows:

$$\begin{aligned}S_{\varepsilon\varepsilon}(s)&=(GW-H)S_\Omega(W_*G_*-H_*)+\\&+(GW-H)S_{\varphi\Omega}G_*+GS_{\Omega\varphi}(W_*G_*-H_*)+\\&+GS_\varphi G_*,\end{aligned} \quad (31)$$

where asterisk designates complex conjugate, $S_{\Omega\varphi}(s)$ and $S_{\varphi\Omega}(s)$ are the cross spectral densities between input angular rate and additive sensor noise, which assumed to be known.

By means of introducing new variables defined as

$$\begin{aligned}DD_*&=WS_\Omega W_*+WS_{\varphi\Omega}+S_{\Omega\varphi}W_*+S_\varphi,\\\Gamma\Gamma_*&=R,\ G_0=\Gamma GD,\\T&=\Gamma H(S_\Omega W_*+S_{\varphi\Omega})D_*^{-1},\end{aligned} \quad (32)$$

and substituting power spectral density (31) into (30), first variation of the performance criterion (30) with respect to the unknown filter related function G_0 will become

$$\delta J=\frac{1}{j}\int_{-j\infty}^{j\infty}[(G_0-T)\delta G_0+\delta G_{0*}(G_{0*}-T_*)]ds. \quad (33)$$

Minimum of the performance criterion (30) is achieved when the first variation (33) turns to zero. Apparently, this is achieved when

$$G=\Gamma^{-1}(T_0+T_+)D^{-1}. \quad (34)$$

Here T_0 is the integer part of the function T, and T_+ is the part of the function T that contains only poles with negative real parts (stable poles) and is the result of the Wiener-Hopf separation procedure.

Using optimal solution (34) and spectral density for the angular rate (27) we can now derive static optimal filter functions for the two cases of the sensor noise (28) and (29). Cross spectral densities between angular rate and noise are assumed to be absent ($S_{\varphi\Omega}(s)=S_{\Omega\varphi}(s)=0$).

After performing transformations according to (32) and renormalizing to remove steady state error, the optimal filter in case of the white sensor noise (28) is found as

$$\begin{aligned}G(s)&=[B\sqrt{1+\gamma^2}\,(s+\zeta k)]/\\/[\gamma s^2&+s\sqrt{\gamma(B^2\gamma+\zeta^2k^2\gamma+2\zeta kB\sqrt{1+\gamma^2})}+\\&+\zeta kB\sqrt{1+\gamma^2}].\end{aligned} \quad (35)$$

In case of the high-pass sensor noise (29), optimal filter is found in the following form:

$$G(s)=\frac{B(s+\zeta k)}{s^2\gamma+s\sqrt{\zeta k\gamma(2B+\zeta k\gamma)}+B\zeta k}. \quad (36)$$

Depending on which of the disturbance model is found to be the most appropriate, either filter (35) or filter (36) should be used.

One should note that obtained optimal filters (35) and (36) are *static*, and being expressed in terms of

transfer functions can be easily implemented using simple analog electronics at a low-level integrated circuitry. Contrary to static filtering, using filtering based on Kalman filter algorithm require microprocessor, which might not be feasible as in terms of cost efficiency as well as not providing sufficiently small high sampling frequency.

Let us now study performances of the obtained optimal sensor noise filters by means of numerical simulations of the realistic CVG. In order to obtain the most realistic simulation results, equations (1) were used to simulate sensitive element dynamics. Secondary oscillations are then synchronously demodulated, and "white" sensor noise is added. Input angular rate is assumed to be in a form of square pulses. Results of numerical simulations of the "white" sensor noise filtering are shown in the figure 5.

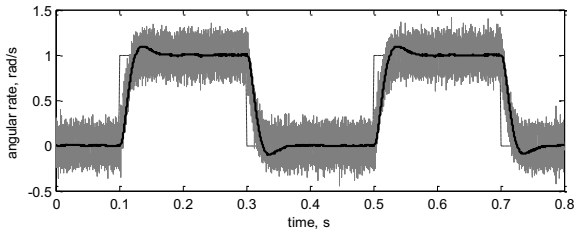

Fig. 5. **Sensor noise filtering simulation**
(dashed – input angular rate, grey – noised output, black – filtered output)

These simulations were carried out for the γ=0.1 and bandwidth of the angular rate B=3 Hz. One should observe good performance of the synthesized filter.

Optimal Kalman filter synthesis

Despite the excellent performance of the Wiener filter in case of the stationary stochastic noises and disturbances, non-stationary noises still would require to use adaptive Kalman filtering along with the corresponding computational hardware.

Let us now demonstrate how to synthesize adaptive Kalman filter using demodulated dynamics of CVG. In order to implement Kalman filter we have to derive difference model of the CVG dynamics in the following form:

$$\begin{cases} X_n = F \cdot X_{n-1} + w_{n-1}, \\ Z_n = C \cdot X_n + v_n. \end{cases} \quad (37)$$

Here X_n is the sampled state vector $X = \{\Omega \quad \Omega_0\}'$, Z_n is the measured state vector, $C = [1 \quad 0]$ is the state measurement matrix, w_n and v_n are the process and sensor noises respectively, and F is the state transition matrix, which can be obtained using well-known ([9]) dependency

$$F = L^{-1}\{(I \cdot s - A)^{-1}\}. \quad (38)$$

Here L^{-1} is the inverse Laplace transformation, A is the system matrix, which in case of the simplified system representation (25) is given as

$$A = \begin{bmatrix} -k\zeta & k\zeta \\ 0 & 0 \end{bmatrix}. \quad (39)$$

Note, that input angular rate Ω_0 in (39) is represented as a random walk (integrated white noise), which is the reason of zeroes in the second row of the matrix A. Substituting (39) into (38) results in

$$F = \begin{bmatrix} e^{-k\zeta t} & 1 - e^{-k\zeta t} \\ 0 & 1 \end{bmatrix}. \quad (40)$$

In order to verify state observability for the simplified model (39), let us calculate observability matrix as

$$Q_O = \begin{bmatrix} C \\ C \cdot F \end{bmatrix} = \begin{bmatrix} 1 & 0 \\ e^{-k\zeta t} & 1 - e^{-k\zeta t} \end{bmatrix}. \quad (41)$$

Observability matrix (41) has full rank equal to 2, which satisfies condition for the state observability.

In order to verify Kalman filter performance the same realistic CVG dynamics simulation is used, as in the previous simulations.

Kalman filter block from the Signal Processing Blockset (Simulink/Matlab) is attached to the already demodulated output rate. Input angular rate has shape of squared pulses with 1 rad/s amplitude. White noise is added to the output rate prior to be fed to the Kalman filter block. Results of the numerical simulations are shown in Fig. 6 and 7.

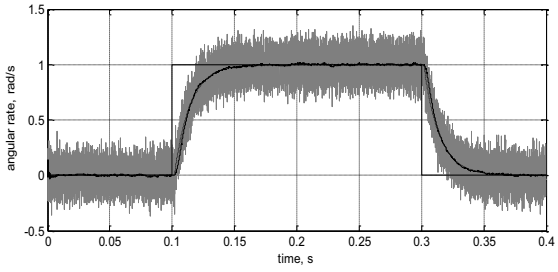

Fig. 6. **Angular rate measurements**
(grey – noised output, dotted – actual output without noise, solid – output estimation)

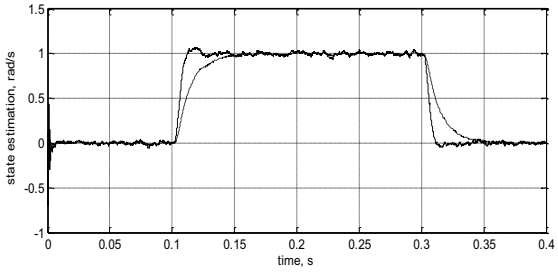

Fig. 7. **State estimations over time**
(solid – input angular rate, dashed – output angular rate)

The following parameters of the CVG were used in simulations: $k = 500Hz$, $\zeta = 0.025$. Zero initial conditions were chosen for the state vector and identity matrix has been used as an initial for the error covariance. Other parameters of the filter are as follows:

$$Q = \begin{bmatrix} 0 & 0 \\ 0 & 2 \cdot 10^{-6} \end{bmatrix}, \; R = 0.01.$$

Analyzing graphs in Fig. 6 and 7 one can see, that added sensor noise has been successfully removed from the output, while input angular rate has been estimated with some errors, however closer to the actual square pulse shape than measured output.

Conclusions

Presented above analysis of CVG dynamics using amplitude-phase complex variables resulted in obtaining system transfer functions, where measured angular rate became an input rather than parameter of the motion equations. This enables analysis of the CVG dynamics in already demodulated signals. More importantly, obtained demodulated transfer functions made possible to apply techniques of the conventional control systems theory to design control systems and optimal filters for CVG. Derived in the paper optimal noise filters using both Wiener and Kalman approaches demonstrated excellent performance in sensor noise removal.

Application of the presented above techniques to CVG sensitive element motion trajectory analysis is viewed as a topic for further research.

References

1. Yazdi N. Micromachined Intertial Sensors / N. Yazdi, F. Ayazi, K. Najafi // Proceedings of the IEEE. – 1998. – Vol. 86, No. 8. – P. 1640-1659.

2. Friedland B. Theory and error analysis of vibrating-member gyroscope / B. Friedland, M. F. Hutton // IEEE Trans. on Automatic Control. – 1978. – no. 23. – P. 545-556.

3. Lynch D. Vibratory gyro analysis by the method of averaging / D. Lynch // Proc. 2nd St. Petersburg Conf. on Gyroscopic Technology and Navigation. – May, 1995. – P. 26-34.

4. Apostolyuk V. Dynamics of Micromechanical Coriolis Vibratory Gyroscopes / V. Apostolyuk, F. Tay // Sensor Letters. – 2004. – Vol. 2, no. 3-4. – P. 252-259.

5. Apostolyuk V. Theory and Design of Micromechanical Vibratory Gyroscopes / V. Apostolyuk // MEMS/NEMS Handbook (Ed: Cornelius T. Leondes), Springer. – 2006. – Vol.1, Chapter 6. – P. 173-195.

6. Leland R. Mechanical Thermal Noise in Vibrating Gyroscopes / R. Leland // Proc. of the American Control Conference. – June 25-27, 2001. – P. 3256-3261.

7. Clark W. Micromachined Vibratory Rate Gyroscopes / W. Clark // PhD Dissertation, U.C. Berkeley. – 1996.

8. Blokhin L. Statistical Dynamics of Control Systems / L. Blokhin, M. Burichenko // Kiev: NAU. – 2003.

9. Bar Shalom Y. Estimation with Applications to Tracking and Navigation / Bar Shalom Y.// Wiley & Sons. – 2003.

Рецензент: д.т.н., проф. О.В. Збруцький, Факультет авіаційних та космічних систем, Національний технічний університет України «КПІ», м. Київ.

ДЕМОДУЛЬОВАНА ДИНАМІКА ТА ОПТИМАЛЬНА ФІЛЬТРАЦІЯ ШУМІВ ДЛЯ КОРІОЛІСОВИХ ВІБРАЦІЙНИХ ГІРОСКОПІВ

В.О. Апостолюк

Аналіз динаміки чутливого елемента коріолісових вібраційних гіроскопів (КВГ) в термінах амплітудно-фазових змінних дозволив отримати відповідні передатні функції таких датчиків, де кутова швидкість є входом системи. Оримані передатні функції було спрощено для декількох спеціальних випадків та використано для отримання полюсів, амплітудно- та фазочастотних характеристик КВГ. Точність отриманих спрощених передатних функцій було проаналізовано та порівняно із точною чисельною моделлю динаміки чутливого елемента. За допомогою отриманих передатних функцій було синтезовано оптимальні фільтри шумів вимірювання методами Вінера та Калмана.

Ключові слова: *вібраційний гіроскоп, динаміка чутливого елемента, оптимальна фільтрація, шуми вимірювання.*

ДЕМОДУЛИРОВАННАЯ ДИНАМИКА И ОПТИМАЛЬНАЯ ФИЛЬТРАЦИЯ ШУМОВ ДЛЯ КОРИОЛИСОВЫХ ВИБРАЦИОННЫХ ГИРОСКОПОВ

В.А. Апостолюк

Анализ динамики чувствительного элемента кориолисовых вибрационных гироскопов (КВГ) в терминах амплитудно-фазовых переменных позволил получить соответствующие передаточные функции таких датчиков, где угловая скорость является входом системы. Полученные передаточные функции были упрощены для нескольких частных случаев и использованы для получения выражений для полюсов, амплитудно- и фазочастотных характеристик КВГ. Точность полученных упрощенных передаточных функций была проанализирована и сравнена с точной численной моделью динамики чувствительного элемента. С помощью полученных передаточных функций были синтезированы оптимальные фильтры шумов измерения методами Винера и Калмана.

Ключевые слова: *вибрационный гироскоп, динамика чувствительного элемента, оптимальная фильтрация, шимы измерения.*